# On the stability and necessary electrophoretic mobility of bare oil nanodroplets in water

Cite as: J. Chem. Phys. **152**, 241104 (2020); https://doi.org/10.1063/5.0009640 Submitted: 02 April 2020 . Accepted: 08 June 2020 . Published Online: 26 June 2020

S. Pullanchery (D, S. Kulik, H. I. Okur (D, H. B. de Aguiar (D, and S. Roke (D









### ARTICLES YOU MAY BE INTERESTED IN

Non-Hermitian quantum mechanics and exceptional points in molecular electronics The Journal of Chemical Physics 152, 244119 (2020); https://doi.org/10.1063/5.0006365

Lock-in Amplifiers up to 600 MHz







# On the stability and necessary electrophoretic mobility of bare oil nanodroplets in water

Cite as: J. Chem. Phys. 152, 241104 (2020); doi: 10.1063/5.0009640

Submitted: 2 April 2020 · Accepted: 8 June 2020 ·

Published Online: 26 June 2020









S. Pullanchery, D. S. Kulik, H. I. Okur, D. H. B. de Aguiar, D. and S. Roke D. D. Pullanchery, D. S. Kulik, D. S. Roke







# **AFFILIATIONS**

- Laboratory for Fundamental BioPhotonics, Institute of Bioengineering (IBI), Institute of Materials Science (IMX) and Engineering, School of Engineering (STI), and Lausanne Centre for Ultrafast Science, École Polytechnique Fédérale de Lausanne (EPFL), CH-1015 Lausanne, Switzerland
- <sup>2</sup>Department of Chemistry and National Nanotechnology Research Center (UNAM), Bilkent University, 06800 Ankara, Turkey
- <sup>3</sup>Laboratoire Kastler Brossel, ENS-Université PSL, CNRS, Sorbonne Université, Collège de France, 24 rue Lhomond, 75005 Paris, France

## **ABSTRACT**

Hydrophobic oil droplets, particles, and air bubbles can be dispersed in water as kinetically stabilized dispersions. It has been established since the 19th century that such objects harbor a negative electrostatic potential roughly twice larger than the thermal energy. The source of this charge continues to be one of the core observations in relation to hydrophobicity, and its molecular explanation is still debated. What is clear though is that the stabilizing interaction in these systems is understood in terms of electrostatic repulsion via Derjaguin, Landau, Verwey, and Overbeek theory. Recent work [A. P. Carpenter et al., Proc. Natl. Acad. Sci. U. S. A. 116, 9214 (2019)] has added another element into the discussion, reporting the creation of bare near-zero charged droplets of oil in neat water that are stable for several days. Key to the creation of the droplets is a rigorous glassware cleaning procedure. Here, we investigate these conclusions and show that the cleaning procedure of glassware has no influence on the electrophoretic mobility of the droplets and that oil droplets with near-zero charge are unstable. We provide an alternative possible explanation for the observations involving glass surface chemistry.

© 2020 Author(s). All article content, except where otherwise noted, is licensed under a Creative Commons Attribution (CC BY) license (http://creativecommons.org/licenses/by/4.0/). https://doi.org/10.1063/5.0009640

Hydrophobicity is key to many interactions and processes in physics, chemistry, and biology. Sub-micrometer sized or nanoscale hydrophobic oil droplets or particles in water form a very important model system for understanding how hydrophobicity works. Since the late 19th/early 20th century, 2-9 hydrophobic nanodroplets and air/gas bubbles have been prepared and investigated. Early experiments<sup>5,7</sup> reported the surprising observation that oil droplets or air bubbles in water move towards a positive electrode when subjected to an electrostatic field. This negative electrophoretic mobility is often converted into a zeta ( $\zeta$ )-potential. The  $\zeta$ -potential is interpreted as the electrostatic potential on the slip plane of a particle or droplet, 10 which is the plane that separates molecules that move with the droplet from molecules that do not.

Figure 1(a) shows a selection of ζ-potential values reported by three different research groups since 1996 who all performed electrophoretic mobility measurements on hexadecane droplets in water. Marinova et al., Creux et al., and Vácha et al. all reported values in the range  $-55 \text{ mV} < \zeta < -71 \text{ mV}$  at pH neutral conditions and dropping to  $-81~\text{mV} < \zeta < -100~\text{mV}$  at pH 9. Recent data were reviewed in Ref. 2 showing a similar result for other hydrophobic liquids as well as gases: A single N2 bubble, air bubbles, <sup>14</sup> nitrobenzene, <sup>6</sup> dodecane, <sup>6</sup> Teflon, <sup>15</sup> octadecane, <sup>16</sup> and hydrogen<sup>17</sup> all show the same behavior, a monotonous decrease in the electrophoretic mobility or ζ-potential as a function of pH. All these published experimental studies agree on the sign and magnitude of the electrophoretic mobility/ζ-potential. The source of this mobility, however, is not known and is still hotly debated. The most frequently given explanations focus around ion adsorption of a specific negatively charged ionic species. The hydroxide ion<sup>3</sup> and the bicarbonate ion<sup>18</sup> are two commonly mentioned

a) Author to whom correspondence should be addressed: sylvie.roke@epfl.ch

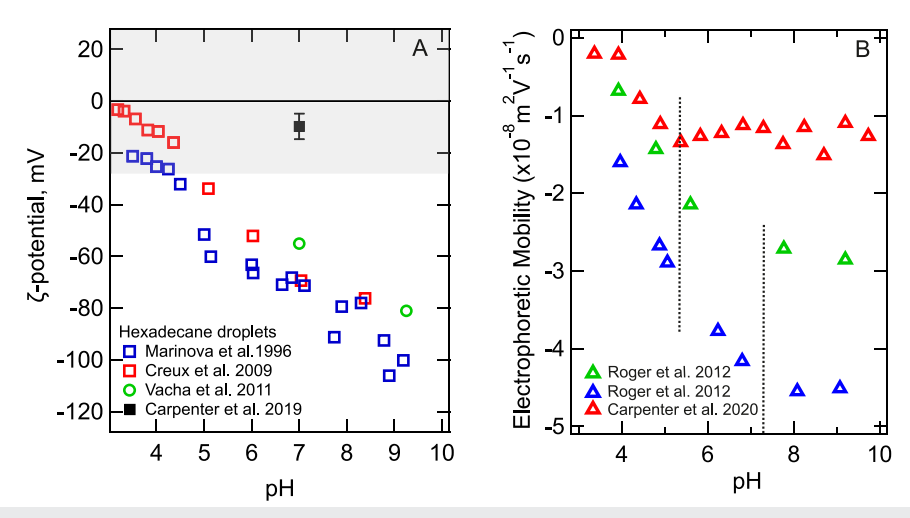


FIG. 1. (a) ζ-potential values of *n*-hexadecane nanodroplets in water collected from three different literature studies.<sup>6,8,9</sup> The gray area represents the region where the electrostatic repulsion is smaller than the thermal energy, leading to unstable dispersions.<sup>11</sup> (b) Electrophoretic mobility values of *n*-hexadecane nanodroplets in water from Ref. 12, showing data from the Richmond lab (red data) and data from a study reported by Roger and Cabane <sup>13</sup> (green and blue data), showing the effects of carboxylic acid impurities in the oil phase. The black dotted lines indicate the difference in chemical equilibrium constant between the green and blue curves and the red curve. Note that the data in panel (a) decrease monotonously, whereas the data in panel (b) have the characteristic shape similar to a surface deprotonation reaction, indicating a different interfacial mechanism.

possibilities. However, since small non-polarizable ions are generally not surface active, <sup>19,20</sup> this is nowadays questioned. Sum frequency scattering studies <sup>9,21</sup> have to date not found any evidence for the adsorption of hydroxide ions (although the complete surface vibrational water spectrum has not been measured), nor do surface tension measurements <sup>22,23</sup> or theoretical studies <sup>19</sup> support this hypothesis.

Another type of explanation focuses on water. Since the hydrogen bond network is asymmetric around a bubble, droplet, or particle, it might be involved in producing a negative electrophoretic mobility via either charge transfer<sup>9,24</sup> or polarizability.<sup>25</sup> What is agreed upon by all these studies is that emulsions or colloidal dispersions cannot be kinetically stable unless the droplets or particles experience a strong repulsive interaction 11,26 explicitly verified theoretically and experimentally. The repulsive force needed to prevent two objects from merging arises from the interactions that are inherent to the system, as dictated by the nature of the chemicals present. For any type of colloidal dispersion, these particleparticle interactions are divided into attractive interactions (van der Waals interactions) and repulsive interactions (electrostatic interactions), and these are combined in Derjaguin, Landau, Verwey, and Overbeek (DLVO) theory. 11,26 In addition, there are also steric repulsion<sup>11,29</sup> and depletion interactions,<sup>11,29</sup> which contribute to the stability of a colloidal dispersion. For a dispersion composed of pure oil droplets, pure gas bubbles, or solid hydrophobic particles suspended in pure water or an electrolyte solution, the latter two interactions are generally not considered relevant. 11 This is simply because there are no bulky polymers or micelles present. Dispersive van der Waals interactions are attractive and will reduce the stability. This renders the electrostatic interactions as the only viable candidate for stabilizing nanoemulsions or other dispersions<sup>11</sup> of pure compounds.

Other explanations have been put forward based on the involvement of impurities in the oil phase. 30-32 A study in 2012 by Roger and Cabane attributed the mobility of oil droplets in water to oil-soluble carboxylate impurities. Figure 1(b) shows this data: the blue curve shows 99% pure oil, while the green curve shows a set with 99.8% pure oil. Indeed, the shape of the curve resembles that of a deprotonation chemical equilibrium, and it is known that some oils may have carboxylic acid impurities, but these can be detected by a Zisman test<sup>33</sup> and removed by passing the oil over an alumina column, which was not done here. Vibrational sum frequency scattering studies in Ref. 34 found no evidence for the surface presence of alkyl carboxylates of oils at the stated surface concentrations. Figures 1(a) and 1(b) display distinctly shaped pH dependencies, suggesting distinct mechanisms. Since different hydrophobic materials display the same trend as in Fig. 1(a), it is unlikely that a specific impurity would be responsible for that behavior.4

Finally, two recent studies contributed by Carpenter et al. 12,35 concluded that nanodroplets of hexadecane can be produced by standard preparation techniques, but by using a proprietary compound, NOCHROMIX®, and a "stringent multi-step glassware cleaning procedure," resulting in the production of "moderately" or "marginally" stable nanoemulsions with near-zero droplet charge. The  $\zeta$ -potential value from the first study in 2019<sup>35</sup> is shown as the black data point in Fig. 1(a), and the electrophoretic mobility recorded as a function of pH<sup>12</sup> is shown in Fig. 1(b). This conclusion casts doubts on a multitude of studies that report the apparent negative charge as an intrinsic property of hydrophobic droplets in water. Formation of nanoemulsions with near-zero charge is quite surprising: It appears to contradict the DLVO derived stability mechanism [the gray shaded area in Fig. 1(a) shows the unstable regime]. Cleanliness has been the topic of a number of debates:4, in relation to the used salts for electrolyte interfacial studies,<sup>36</sup>

concerning the purity of oils when preparing nanoemulsions,  $^{4.13,34}$  or in relation to surface tension measurements  $^{37}$  and in particular the Jones–Ray effect.  $^{38,39}$  All of these studies deal with the concern of the purity of chemicals. Impurities, whether in water, oil, or on the surface of glass, are generally chemically different depending on the history of the chemicals and sample treatment. Yet, despite the large diversity of cleaning and storage procedures, different research groups  $^{3.5,7-9,21,34,40,41}$  have consistently reported reproducible electrophoretic mobility or  $\zeta$ -potential values (Fig. 1, Refs. 2 and 3 for older data), suggesting that charged surface active impurities arising from improper glassware cleaning are not the main source of the observation.

In this work, we therefore investigate nanodroplet mobility and stability paying close attention to the glassware cleaning procedure. We clean glassware with the proprietary compound NOCHROMIX® as suggested by Carpenter et al. 12,35 but also vary the prescribed cleaning agent using more commonly used non-proprietary ones and prepared nanoemulsions of pure hexadecane in pure water. We report electrophoretic mobility and ζ-potential values and show that the cleaning agent of the glassware has no significant influence on the electrophoretic mobility. We also deliberately produced near-zero charged oil droplets in water and demonstrate that such nanoemulsions are unstable, displaying droplets coalescing within minutes after preparation. We discuss different aspects of electrophoretic mobility measurements as well as their use in relation to understanding the properties of nanodroplets. Finally, based on our data and the data provided in the Richmond laboratory studies of Refs. 12 and 35, we propose an alternative mechanism for the reduced  $\zeta$ -potential that can result from prolonged acid treatment of the surface of the used glassware.

Zeta-potential and stability of oil nanodroplets in water. To investigate the conclusions drawn in Refs. 12 and 35, we prepared nanoemulsions according to the following protocol. The glassware used for preparing nanoemulsions was freshly taken out of the manufacturer's packaging and never re-used after the preparation. As a first step, all glassware used to prepare and store the solutions and samples was cleaned according to one of the three different cleaning methods: (1) glassware was soaked in a freshly prepared piranha solution [3:1 H<sub>2</sub>SO<sub>4</sub> (95%-97%, Merck) and H<sub>2</sub>O<sub>2</sub> (30%, Reactolab SA)] for ~45 min and subsequently rinsed with copious amounts of ultrapure water prior to use; (2) glassware was soaked in a freshly prepared NOCHROMIX®:H2SO4 (GODAX Laboratories, Inc.) mixture that is mixed based on the provided instructions, followed by thoroughly rinsing with ultrapure water to remove acidic components from the glass surface; and (3) glassware was cleaned with a Deconex® (Borer Chemie AG) solution prepared by 1:20 dilution with ultrapure water, then sonicated for an hour (using a reduced power compared to what is needed to prepare emulsions), and subsequently washed and rinsed at least ten times with MilliQ water. Ultrapure H<sub>2</sub>O with an electric resistance of 18.2  $M\Omega$  cm was obtained from a Milli-Q UF-Plus instrument (Millipore, Inc.). For experiments with heavy water, the D2O used was 99.8% D atoms with an electrical resistance of >2 M $\Omega$  cm (Armar). We used n-hexadecane (Sigma-Aldrich, analytical standard) with highest commercially available purity purchased in quantities <5 ml and tested the purity of it with a Zisman test. 33,42 We also tested if further purification of the hexadecane phase had any effect on emulsion quality, inspired by previous experiments showing the effect of purity on surface tension experiments.  $^{37,38}$  For these tests, hexadecane was purified by running it several times through an activated alumina (Sigma-Aldrich) column, which was preprocessed by heating to  $500\,^{\circ}$ C for 2 h. Such processed n-hexadecane gives rise to identical nanoemulsion samples and identical results to the Zisman test with the samples using the commercially available highest purity n-hexadecane.

The dispersions of nanometer-sized oil droplets in H<sub>2</sub>O [Fig. 1(a)] or mixtures of H<sub>2</sub>O and D<sub>2</sub>O (Fig. 2) were prepared with 1 vol. %-2 vol. % of the dispersed phase in the continuous phase. The dispersions were mixed for 2 min with a hand-held homogenizer (TH, OMNI International) with an angular velocity of 300 rpm or vortexed for 3 min (IKAR) Vortex 2) and then placed in an ultrasonic bath (35 kHz, 400 W, Bandelin) until a monodisperse sample was formed (<5 min). Alternatively, the nanodroplets could be formed by sonication alone using the same sonicator but with significantly longer sonication times. For stable samples, the droplet diameter was consistently found to have a mean value in the range of 130 nm-230 nm with a polydispersity index (PDI) < 0.3. The size of each final sample was monitored every few minutes of the sonication process. All samples were stored and measured in sealed cuvettes, and all measurements were performed at 25 °C. The pH values of the solutions were measured using a pH-meter (HI 5522 pH/ISE/EC bench meter and HI 1330 pH electrode, Hanna Instruments) calibrated with the appropriate buffer solutions. Conductivity values were obtained using a HI 5522 pH/ISE/EC bench meter and HI 76312 conductivity electrode (Hanna Instruments) calibrated with the appropriate buffer solutions to verify the ionic strength of the solutions.

The size distribution of the droplets was measured with dynamic light scattering (DLS) using a Malvern ZS nanosizer instrument. The hydrodynamic diameter was calculated from the intensity autocorrelation function using the optical properties of the liquids. The electrophoretic mobility measurements were performed using laser Doppler velocimetry and phase analysis light scattering, employing the same instrument (Malvern ZS nanosizer). To perform the electrophoretic mobility, the nanoemulsions were diluted to 0.02 vol. % by adding ultrapure water. We used two such instruments in different laboratories. The electrophoretic mobility ( $\mu$ ) values were converted into  $\zeta$ -potential ( $\zeta$ ) values using the following expression:  $\mu = \frac{\varepsilon \varepsilon_0}{\eta} \zeta f(\kappa a)$ , where  $\varepsilon_0$  is the vacuum permittivity,  $\varepsilon$ is the relative permittivity of water,  $\eta$  is the viscosity of the used liquid,  $f(\kappa a)$  is Henry's function,  $\kappa$  is the inverse Debye length  $(\kappa^{-1} = \sqrt{\varepsilon_0 \varepsilon k_B T / 2 \cdot 10^3 N_A e^2 I}$ , where  $k_B$  is the Boltzmann constant, T is the temperature,  $N_A$  is Avogadro's number, e is the elementary charge, and I is ionic strength), and a is the radius of the droplet. Henry's function has two solutions that are generally used in the software of the DLS instrument, namely, for  $\kappa a \to \infty$ ,  $f(\kappa a) \to 1$ , resulting in the well-known Smoluchowski formula, or if  $\kappa a \rightarrow 0$ ,  $f(\kappa a) \rightarrow 2/3$ , leading to the well-known Hückel formula. However, in the case of nanoemulsion droplets, one may find  $\kappa a$  values in the range outside those two limiting cases, and one has to use a more complicated expression for  $f(\kappa a)$ . Ohshima proposed the following approximation for this case:

$$f(\kappa a) = \frac{2}{3} \left[ 1 + \frac{1}{2\left\{1 + \frac{2.5}{\kappa a(1 + 2e^{-\kappa a})}\right\}^3} \right]$$
, which we use.

Figure 2(a) shows the converted  $\zeta$ -potential values for nanoemulsions prepared using the three different glassware cleaning procedures. Measurements were made in ninefold on the two instruments from the two different laboratories (represented by the black and the blue symbols). It can be seen that the nature of the glassware cleaning agent used to prepare the nanoemulsions has no significant influence on the final  $\zeta$ -potential value. The size distribution of one of the prepared droplet systems is shown in Fig. 2(b) (black), depicting the dynamic light scattering intensity distribution. Nanoemulsions prepared with such  $\zeta$ -potential values are generally stable: The inset in Fig. 2(b) shows the DLS size distribution of the same sample right after preparation and 18 days after preparation.

Next, we investigate the effect of having a "near-zero charge," meaning "a  $\zeta$ -potential of  $-10 \pm 5$  mV, with some samples having measured  $\zeta$ -potential values within an error of zero" on the oil droplets' stability. We started with a freshly prepared nanoemulsion at pH neutral conditions ( $\zeta = -56$  mV). We then reduced the pH of the solution such that the  $\zeta$ -potential reached a value of -10 mV. Figure 2(b) shows the intensity weighted size distribution as measured with DLS directly after preparing the nanodroplets, adding HCl solution and determining the  $\zeta$ -potential (this procedure took <5 min in total). The effect of the reduced magnitude in  $\zeta$ -potential is clear: the droplets become immediately unstable as quantified by the broadening in the size distribution and appearance of droplets that are up to several micrometers in size.

In Refs. 12 and 35, near-zero charged oil droplets were studied with sum frequency scattering (SFS). The recording time of this SFS experiment is 210 min, <sup>12,35</sup> and additional time to insert the sample and fine-tune the optical alignment is probably needed as well. As a consequence, we expect that the SFS data in Refs. 12 and 35 report on a droplet ensemble that changes in size, number density, and potentially also surface structure during the measurement. Previous SFS

studies have shown that SFS spectra as well as SFS patterns change when particles aggregate in a dispersion. However, the SFS spectra are used as key evidence for the impurity hypothesis  $^{12,35}$  because of the following observations: In Figs.  $3^{35}$  and  $4,^{12}$  a shoulder peak with a center frequency and full width at half maximum (FWHM) of 2688 cm $^{-1}$  and  $\sim\!55$  cm $^{-1}$ , respectively, is present and concluded to arise from non-interacting O-D oscillators. Nanodroplets with >10  $\mu$ M of the sodium dodecyl sulfate (SDS) surfactant in the dispersion do not show this peak (Fig. S5),  $^{35}$  leading to the interpretation that SDS has fully covered the surface and suppressed the free O-D groups (Fig.  $^{35}$ ). This conclusion is inspired by previous sum frequency generation (SFG) studies on the planar CCl4/water interface. These SFG spectra of water were found to be sensitive to the addition of nanomolar amounts of SDS.

In our opinion, there are several unsupported elements in this reasoning. First, the changes observed in the planar CCl<sub>4</sub>/water study occur primarily in the low frequency side of the spectra, involving hydrogen bonded water. The high frequency peak at ~3670 cm<sup>-1</sup> does not change its intensity with added SDS. Second, although the peak at 2688 cm<sup>-1</sup> shares some similarity with a non-bonded O-D mode, the width and frequency are not matching well. A 50% H<sub>2</sub>O:D<sub>2</sub>O SFG spectrum of the air/water interface has peaks at 2725 cm<sup>-1</sup> and 2745 cm<sup>-1</sup> with widths of 10 cm<sup>-1</sup> and 14 cm<sup>-1</sup>, respectively (Fig. 3<sup>46</sup>). Was this peak to be found in an SFS spectrum, symmetry dictates that it should be most intense in the SSP polarization combination, not in the PPP polarization<sup>21</sup> as was measured by Carpenter et al. 12,35 Other unexplained features relate to surface to volume ratio arguments:  $10 \,\mu\mathrm{M}$  of impurities will, under the most favorable conditions of complete surface adsorption (with the assumption of a projected surface area of 0.5 nm<sup>2</sup> per SDS molecule), cover ~1.5% of the available droplet surface area (150 nm radius, 1 vol. %). There is no reason why this would lead to a full suppression of OD groups on the surface.<sup>47</sup> Furthermore, in our

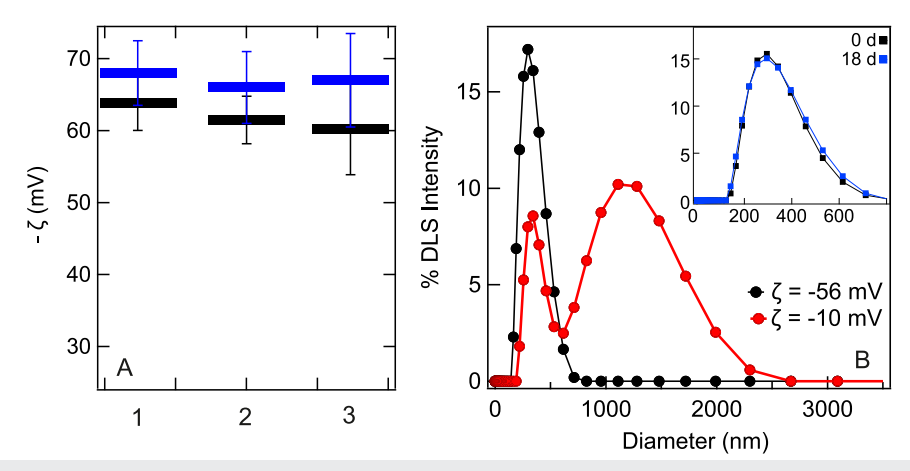


FIG. 2. Cleaning procedure and stability of nanodroplets. (a) ζ-potentials for 0.02 vol. % hexadecane nanoemulsions prepared using glassware cleaned with three different methods. 1–3 refer to glassware cleaning with piranha, NOCHROMIX®, and Deconex® solutions, respectively. The blue and black data are measurements performed with different instruments. The values of electrophoretic mobility averaged between two instruments (and corresponding diameter) are  $-3.1 \times 10^{-8} \text{ m}^2 \text{ V}^{-1} \text{ s}^{-1}$  (200 nm) for Piranha-cleaning,  $-3.0 \times 10^{-8} \text{ m}^2 \text{ V}^{-1} \text{ s}^{-1}$  (180 nm) for NOCHROMIX®-cleaning, and  $-3.0 \times 10^{-8} \text{ m}^2 \text{ V}^{-1} \text{ s}^{-1}$  (156 nm) for Deconex®-cleaning. (b) Distribution of size for nanodroplets prepared at pH neutral conditions (black data). Within ~5 min after reducing the ζ-potential to -10 mV, the DLS size distribution changes drastically (red curve), indicating a highly unstable sample. Inset: (a) stable sample right after preparation (black data) and 18 days later (blue data).

previous experiments<sup>39</sup> we determined the trace amount of organic content in our aqueous glass stored solutions to be on the order of nM—three orders of magnitude lower than suggested. Finally, glass is a non-equilibrium compound that is fabricated by calcination at >500 °C.<sup>38</sup> As a consequence, organic trace impurities will likely be removed from the glass surface by this process, so they are not likely to be the main source of glass impurity. Therefore, it is difficult to imagine how negatively charged organic surfactant type of impurities might be present on the glass in such high concentrations.

The effect of prolonged acid baths and sonication. For these reasons, we suggest a possible alternative mechanism for the observation that "the creation of low charge nanoemulsions was found to be sensitive to the storage conditions of the aqueous phase and glassware cleaning procedures." Figure 3 provides an illustration of the mechanism.

Besides the use of cleaning agent, another difference that stands out is the duration of the glass cleaning treatment. Carpenter et al. 12,35 state, "Glassware was first copiously rinsed and then soaked in a preliminary acid bath consisting of concentrated sulfuric acid mixed with NOCHROMIX (Godax Labs, Inc.) for at least 12 h. This glassware was then rinsed using ultrapure water and placed in a second, "isolated," acid bath that also contained concentrated sulfuric acid and NOCHROMIX. After 24 h in the isolated acid bath, all glassware was rinsed with copious amounts of ultrapure water." Exposure of glass to pH 0 conditions drastically changes the surface of the glass. This type of glass etching turns a smooth surface into a severely roughened surface with roughness on the order of several tens to hundreds of nanometers. 49 Under pH 0 conditions, glass dissolves at a rate of 1 g/m<sup>2</sup>d-100 g/m<sup>2</sup>d,<sup>51</sup> leading to a substantial amount of dissolved material (equivalent to ~9 mM-0.9 M of the material in a 4 ml vial). Figure 3 shows AFM images from Ref. 49 of a glass surface before treatment (left panel), after 30 min boiling in 50% H<sub>2</sub>SO<sub>4</sub> (middle panel), and sonication for 30 min (right panel). Although rinsing influences the protonation equilibrium, it does not revert the surface back to its original state. The kinetics of acid-base chemistry of glass is slow<sup>51-53</sup> and strongly dependent on the type of glass employed and the history of the sample. Thus, the damaged glass consisting of a roughened surface and potentially multiple layers with different amounts of water content will continue to leach positively charged species as well as silicates<sup>54</sup> when placed in an aqueous solution (Fig. 3, middle panel). Upon sonication, nanosized glass particles, polymeric silicates, and positively charged surface species will detach from the surface,<sup>52</sup> which is seen in the AFM image (right panel) of Fig. 3. These species may participate in the emulsification process and modify the electrophoretic mobility as well as the SFS spectrum. Furthermore, a striking difference between the pH dependence in Fig. 1(b) (red curve)<sup>12</sup> and the data in Fig. 1(a) suggests that a deprotonation reaction is playing a role (with the inflection point of the data highlighted by a vertical line). The trend of the deprotonation reaction of the red curve in Fig. 1(b) is similar to that of silica nanoparticles in water. 55 We note that this is only a possible mechanism because details such as the type of glass used, the type of sonicator, the duration of the sonication process, and the power used in the sonication are all relevant but unknown to us.

Summarizing, we showed that bare oil droplets in neat water (nanoemulsions) are stable only when the electrophoretic mobility is high enough to ensure the absence of coagulation by means of sufficiently large electrostatic repulsion, in agreement with earlier experiments  $^{28}$  and theory.  $^{27}$  The  $\zeta\text{-potential}$  values derived from the mobility measurements are in the range of  $\sim$  -50 mV >  $\zeta$  > -80 mV and are in good agreement with decades of literature reports. The cleaning procedure of the used glassware has no influence on the eventual  $\zeta$ -potential value. Bringing the  $\zeta$ -potential magnitude down to a value less than the thermal energy results in unstable droplets with large variations in size distribution. Finally, we propose an alternative explanation for the observed phenomena by Carpenter et al. 12,35 based on the influence of prolonged etching and subsequent ultrasonication on glass chemistry. These results reduce the complexity of the nature of hydrophobicity to the following question: "What is the molecular source of charge on hydrophobic particles, droplets, and bubbles dispersed in water?" To answer this question, more sophisticated measurements are necessary than recording the electrophoretic mobility as a function of pH. With the ongoing development of interfacial nonlinear optical techniques such as sum frequency scattering of a wide spectral range,<sup>5</sup> angle-resolved second harmonic scattering to measure surface potentials,<sup>57</sup> and molecular modeling, new insights are potentially within reach.

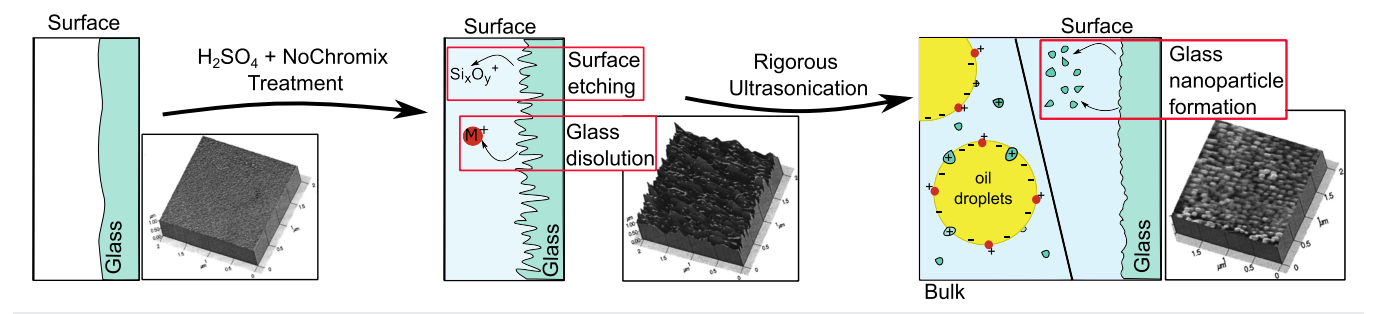


**FIG. 3**. Surface chemistry of glass during acid treatment. Schematic illustration of glass surface dissolution and etching during prolonged acid treatment and subsequent ultra-sonication. The insets show AFM images taken from Ref. 49, which were made of a clean glass surface (left), a glass surface treated with heated 50% H<sub>2</sub>SO<sub>4</sub> aqueous solution, and the same surface after sonication. The species that detach from the glass surface during sonication participate in the emulsification process and alter the oil droplet surface chemistry. Note that the treatment of the glass does not exactly follow the protocol of Carpenter *et al.*,  $^{12,35}$  as the duration is much shorter. This should be negated by the heating, however. Other types of acid treatments can be found in Ref.  $^{50}$ , all leading to surface etching.

### **ACKNOWLEDGMENTS**

S.R. acknowledges the Julia Jacobi Foundation and the Swiss National Science Foundation (Grant No. 200021-182606-1). H.I.O. thanks EU MCSA-IF (Grant No. 899088) for financial support. H.B.d.A. was supported by the LabEx ENS-ICFP (Grant No. ANR-10-LABX-0010/ANR-10-IDEX-0001-02 PSL).

### **DATA AVAILABILITY**

The data that support the findings of this study are available from the corresponding author upon reasonable request.

### REFERENCES

- <sup>1</sup> P. Ball, Chem. Rev. **108**, 74 (2008).
- <sup>2</sup>N. Agmon et al., Chem. Rev. 116, 7642 (2016).
- <sup>3</sup> J. K. Beattie and A. M. Djerdjev, Angew. Chem., Int. Ed. 43, 3568 (2004).
- <sup>4</sup>J. K. Beattie and A. Gray-Weale, Angew. Chem., Int. Ed. 51, 12941 (2012).
- <sup>5</sup>J. C. Carruthers, Trans. Faraday Soc. **34**, 300 (1938).
- <sup>6</sup>P. Creux et al., J. Phys. Chem. B 113, 14146 (2009).
- <sup>7</sup>W. Dickinson, Trans. Faraday Soc. **37**, 140 (1941).
- <sup>8</sup>K. G. Marinova et al., Langmuir 12, 2045 (1996).
- <sup>9</sup>R. Vácha et al., J. Am. Chem. Soc. 133, 10204 (2011).
- <sup>10</sup>R. J. Hunter, Zeta Potential in Colloid Science (Academic Press, London, 1981).
- <sup>11</sup>R. J. Hunter, Introduction to Modern Colloid Science (Oxford University Press, Oxford, 1993).
- <sup>12</sup> A. P. Carpenter et al., J. Phys. Chem. B **124**, 4234 (2020).
- <sup>13</sup> K. Roger and B. Cabane, Angew. Chem. **124**, 5723 (2012).
- <sup>14</sup>M. Takahashi, J. Phys. Chem. B **109**, 21858 (2005).
- <sup>15</sup>R. Zimmermann, S. Dukhin, and C. Werner, J. Phys. Chem. B **105**, 8544 (2001).
- <sup>16</sup>J. Jabloński, W. Janusz, and J. Szczypa, J. Dispersion Sci. Technol. 20, 165 (1999).
- <sup>17</sup>C. Yang et al., J. Colloid Interface Sci. **243**, 128 (2001).
- <sup>18</sup> X. B. Yan et al., J. Phys. Chem. Lett. **9**, 96 (2018).
- <sup>19</sup>P. Jungwirth and D. J. Tobias, Chem. Rev. **106**, 1259 (2006).
- <sup>20</sup>P. Jungwirth and B. Winter, Annu. Rev. Phys. Chem. **59**, 343 (2008).
- <sup>21</sup> J.-S. Samson et al., Chem. Phys. Lett. **615**, 124 (2014).
- <sup>22</sup> J. K. Beattie et al., J. Colloid Interface Sci. 422, 54 (2014).
- <sup>23</sup>P. K. Weissenborn and R. J. Pugh, J. Colloid Interface Sci. **184**, 550 (1996).

- <sup>24</sup>E. Poli, K. H. Jong, and A. Hassanali, Nat. Commun. 11, 901 (2020).
- <sup>25</sup>D. V. Matyushov, Mol. Phys. **112**, 2029 (2014).
- <sup>26</sup>E. J. W. Verwey, J. T. G. Overbeek, and K. Van Nes, *Theory of the Stability of Lyophobic Colloids: The Interaction of Sol Particles Having an Electric Double Layer* (Elsevier, Amsterdam, 1948).
- <sup>27</sup>D. J. Bonthuis *et al.*, Langmuir **26**, 12614 (2010).
- <sup>28</sup> R. W. O'Brien, J. K. Beattie, and A. M. Djerdjev, J. Colloid Interface Sci. 420, 70 (2014).
- <sup>29</sup>D. J. McClements, Crit. Rev. Food Sci. Nutr. **47**, 611 (2007).
- <sup>30</sup>T. T. Duignan et al., J. Chem. Phys. **149**, 194702 (2018).
- <sup>31</sup>E. Scoppola et al., Molecules **24**, 4113 (2019).
- <sup>32</sup>Y. Uematsu, D. J. Bonthuis, and R. R. Netz, <u>Langmuir</u> **36**, 3645 (2020).
- 33 W. C. Bigelow, D. L. Pickett, and W. A. Zisman, J. Colloid Sci. 1, 513 (1946).
- 34 K. C. Jena, R. Scheu, and S. Roke, Angew. Chem., Int. Ed. 51, 12938 (2012).
- <sup>35</sup> A. P. Carpenter et al., Proc. Natl. Acad. Sci. U. S. A. **116**, 9214 (2019).
- <sup>36</sup>Z. Huang et al., J. Phys. Chem. A 117, 13412 (2013).
- <sup>37</sup>K. Lunkenheimer, H. J. Pergande, and H. Krüger, Rev. Sci. Instrum. 58, 2313 (1987).
- <sup>38</sup>H. I. Okur et al., J. Phys. Chem. Lett. **9**, 6739 (2018).
- <sup>39</sup>H. I. Okur et al., Chem. Phys. Lett. **684**, 433 (2017).
- <sup>40</sup>H. B. de Aguiar et al., J. Am. Chem. Soc. **132**, 2122 (2010).
- <sup>41</sup>E. Zdrali et al., J. Chem. Phys. **150**, 204704 (2019).
- <sup>42</sup>J. P. R. Day and C. D. Bain, Phys. Rev. E: Stat., Nonlinear, Soft Matter Phys. 76, 041601 (2007).
- <sup>43</sup>H. Oshima, J. Colloid Interface Sci. **168**, 269 (1994).
- <sup>44</sup>J. I. Dadap, H. B. de Aguiar, and S. Roke, J. Chem. Phys. **130**, 214710 (2009).
- <sup>45</sup>L. F. Scatena and G. L. Richmond, J. Phys. Chem. B **108**, 12518 (2004).
- <sup>46</sup>I. V. Stiopkin *et al.*, Nature **474**, 192 (2011).
- <sup>47</sup>E. Tyrode et al., J. Phys. Chem. C 111, 11642 (2007).
- <sup>48</sup>J. W. Evans and L. C. De Jonghe, *The Production and Processing of Inorganic Materials* (Springer, Cham, 2016).
- 49 H. K. Jang et al., J. Vac. Sci. Technol., A 18, 401 (2000).
- <sup>50</sup>L. D. Eske and D. W. Galipeau, Colloids Surf., A **154**, 33 (1999).
- <sup>51</sup>D. Strachan, Geochim. Cosmochim. Acta **219**, 111 (2017).
- <sup>52</sup>M. Löbbus et al., Langmuir **14**, 4386 (1998).
- <sup>53</sup> A. Seidel *et al.*, Solid State Ionics **101-103**, 713 (1997).
- <sup>54</sup> A. Ledieu *et al.*, J. Non-Cryst. Solids **343**, 3 (2004).
- <sup>55</sup>K.-M. Kim *et al.*, Int. J. Nanomed. **9**(Suppl. 2), 29 (2014).
- <sup>56</sup>E. Zdrali et al., J. Phys. Chem. B **123**, 2414 (2019).
- <sup>57</sup> A. Marchioro *et al.*, J. Phys. Chem. C **123**, 20393 (2019).